

# Investigation of production routes for the $^{161}\text{Ho}$ Auger-electron emitting radiolanthanide, a candidate for therapy

F. Tárkányi · F. Ditrói · A. Hermanne · S. Takács · A.V. Ignatyuk

Received: 2012-11-13 / Accepted: 2012-12-19

**Abstract** The radiolanthanide  $^{161}\text{Ho}$  (2.48 h) is a promising Auger-electron emitter for internal radiotherapy that can be produced with particle accelerators. The excitation functions of the  $^{nat}\text{Dy}(p,xn)^{161}\text{Ho}$  and  $^{nat}\text{Dy}(d,x)^{161}\text{Ho}$  reactions were measured up to 40 and 50 MeV respectively by using the stacked foil activation method and  $\gamma$ -ray spectrometry. The experimental data were compared with results of the TALYS code available in the TENDL 2011 library [1]. The main parameters of different production routes are discussed.

**Keywords** medical radioisotopes · therapeutical isotopes · proton and deuteron irradiation ·  $^{161}\text{Ho}$  ·  $^{162m}\text{Ho}$

## 1 Introduction

The radiolanthanide  $^{161}\text{Ho}$  is an Auger-electron emitter having also low energy photons in high abundance. It is very suitable for internal radiotherapy of small tumors because of the low energy electrons emitted. The short range of Auger electrons however requires that labeled compounds approach the cell nucleus. It is also interesting as low-energy narrow-band X-ray source for

internal irradiation [2, 3, 4, 5, 6]. Different routes exist to produce  $^{161}\text{Ho}$  with particle accelerators. One route is  $\alpha$ - or  $^3\text{He}$ - particle irradiation of  $^{159}\text{Tb}$  relying on the  $^{159}\text{Tb}(\alpha, 2n)^{161}\text{Ho}$  and  $^{159}\text{Tb}(^3\text{He}, n)^{161}\text{Ho}$  reactions. Another route is the irradiation of dysprosium targets using protons via the  $^{161}\text{Dy}(p, n)$ ,  $^{162}\text{Dy}(p, 2n)$  or deuterons via  $^{160}\text{Dy}(d, n)$  and  $^{161}\text{Dy}(d, 2n)$  reactions. When using the  $^{159}\text{Tb}(\alpha, 2n)^{161}\text{Ho}$ ,  $^{162}\text{Dy}(p, 2n)$  or  $^{161}\text{Dy}(d, 2n)$  reactions processes, emission of one neutron also takes place resulting in simultaneous production of  $^{162}\text{Ho}$ , which is a radionuclide impurity. This radionuclide has a short half-life ground state  $^{162g}\text{Ho}$  (15 min,  $I^\pi = 1^+$ ) and a longer-lived isomeric state (67.0 min,  $I^\pi = 6^-$ ). From the point of view of  $^{161}\text{Ho}$  production, the contamination with the longer-lived excited state has some importance at the beginning after EOB, which will be reduced by the waiting time. The decay through internal transition of  $^{162m}\text{Ho}$  is followed only by low energy low intensity  $\gamma$ -ray emission, but the 38% electron capture decay results in strong high energy  $\gamma$ -lines (see Table 1). The cross-sections of the  $^{159}\text{Tb}(\alpha, 2n)^{161}\text{Ho}$  reaction was investigated by several authors (see in comparison of production routes). Although the basic cross-section data are still missing the proton induced reaction was also used for practical production [5]. The deuteron induced reaction was not used yet for the production and no cross-section data were published. We decided to investigate the excitation functions of the proton and deuteron routes experimentally. Naturally occurring dysprosium is composed of 7 stable isotopes ( $^{156}\text{Dy}$  - 0.06%,  $^{158}\text{Dy}$  - 0.10%,  $^{160}\text{Dy}$  - 2.34%,  $^{161}\text{Dy}$  - 18.9%,  $^{162}\text{Dy}$  - 25.5%,  $^{163}\text{Dy}$  - 24.9% and  $^{164}\text{Dy}$  - 28.2%). Taking into account that many of these stable Dy isotopes have a larger mass number than  $^{161}\text{Ho}$ , the direct experimental investigation of the  $^{161}\text{Dy}(p, n)$ ,  $^{161}\text{Dy}(d, 2n)$  or  $^{160}\text{Dy}(d, n)$  reactions, and routes leading

F. Ditrói F. Tárkányi · S. Takács  
Institute of Nuclear Research of the Hungarian Academy of Sciences  
Tel.: +36-52-509251  
Fax: +36-52-416181  
E-mail: ditroi@atomki.hu

A. Hermanne  
Cyclotron Laboratory, Vrije Universiteit Brussel (VUB),  
Brussels, Belgium

A.V. Ignatyuk  
Institute of Physics and Power Engineering (IPPE), Obninsk  
249020, Russia

**Table 1** Main experimental parameters

Reaction	$^{nat}\text{Dy}(p,x)$	$^{nat}\text{Dy}(d,x)$
Incident particle	Proton	Deuteron
Method	Stacked foil	Stacked foil
Target and thickness	$^{nat}\text{Dy}$ foil, 100.59 $\mu\text{m}$	$^{nat}\text{Dy}$ foil, 100.59 $\mu\text{m}$
Number of target foils	15	15
Accelerator	CGR 560 cyclotron of Vrije Universiteit Brussels	Cyclone 90 cyclotron of the Universit Catholique in City-place Louvain la Neuve (LLN)
Primary energy	36 MeV	50 MeV
Irradiation time	71 min	30 min
Beam current	61 nA	120 nA
Monitor reaction, [recommended values]	$^{nat}\text{Ti}(p,x)^{48}\text{V}$ reaction [12]	$^{27}\text{Al}(d,x)^{24}\text{Na}$ reaction [12]
Monitor target and thickness	$^{nat}\text{Ti}$ , 10.9 $\mu\text{m}$	$^{nat}\text{Al}$ , 26.96 $\mu\text{m}$
detector	HpGe	HpGe
$\gamma$ -spectra measurements	3 series	3 series
Cooling times	1.5 h, 20 h, 80 h	4h, 20h, 120h

to possibly disturbing activation products, should require highly enriched targets. A second possibility is to use natural targets and to use results of theoretical calculations to separate the contributions of the different target isotopes. This supposes an accurate predictivity of the calculations and a method to check the reliability has to be implemented. We adopted this approach by making measurement of production cross-section of  $^{161}\text{Ho}$  on  $^{nat}\text{Dy}$  target with protons and deuterons and by comparing our experimental data with the predictions of the theoretical model codes. In case of good agreement we can then compare the different charged particle production routes using theoretical results validated by integral experiment.

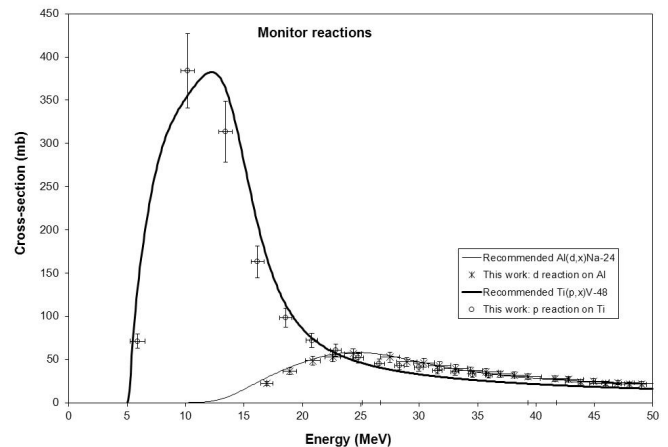
## 2 Experimental and data evaluation

The general characteristics and procedures for irradiation, activity assessment and data evaluation (including estimation of uncertainties) were similar as in our many earlier works [7, 8, 9, 10, 11]. The main experimental parameters for the present study including the chosen monitor reactions [12] are summarized in Table 1. The main methods used in data evaluation and the used decay data [8, 13, 14, 15, 16, 17, 18, 19, 20] are collected in Table 2 and Table 3. The excitation function of simultaneously measured proton and deuteron monitor reactions and comparison with recommended values are shown in Fig. 1.

## 3 Results

### 3.1 Cross-sections

The measured excitation functions for  $^{nat}\text{Dy}(p,x)^{161,162m}\text{Ho}$  and  $^{nat}\text{Dy}(d,x)^{161,162m}\text{Ho}$  are shown in Figs 2-3 and 5-6 in comparison with the results of the model

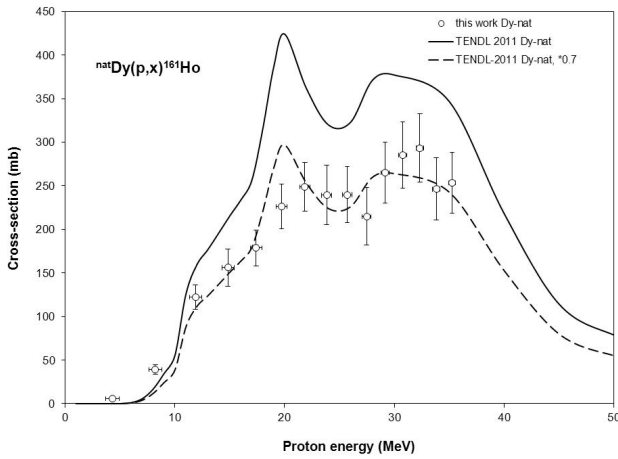
**Fig. 1** The simultaneously measured monitor reactions for determination of proton beam energy and intensity**Table 2** Main parameters of data evaluation (with references)

$\gamma$ -spectrum evaluation	Genie 2000, Forgamma	[13, 14]
Determination of beam intensity	Faraday cup (preliminary) Fitted monitor reaction (final)	[15]
Decay data	NUDAT 2.6	[16]
Reaction Q-values	Q-value calculator	[17]
Determination of beam energy	Andersen (preliminary) Fitted monitor reaction (final)	[18]
Uncertainty of energy	cumulative effects of possible uncertainties	[19]
Cross-sections	Isotopic cross section	[20]
Uncertainty of cross-sections	Sum in quadrature of all individual contributions	[19]
Yield	Physical yield	[20]

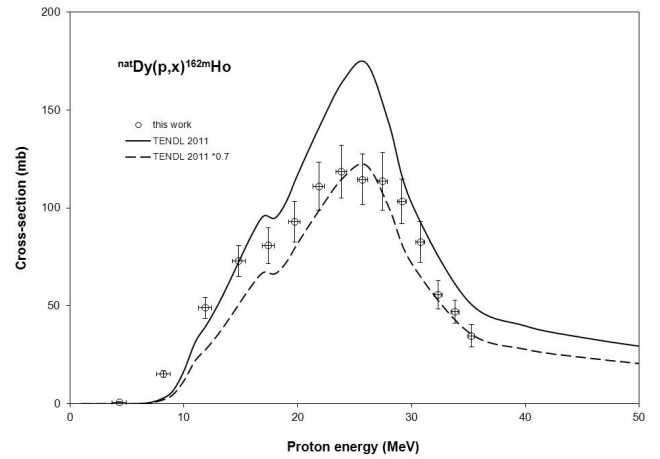
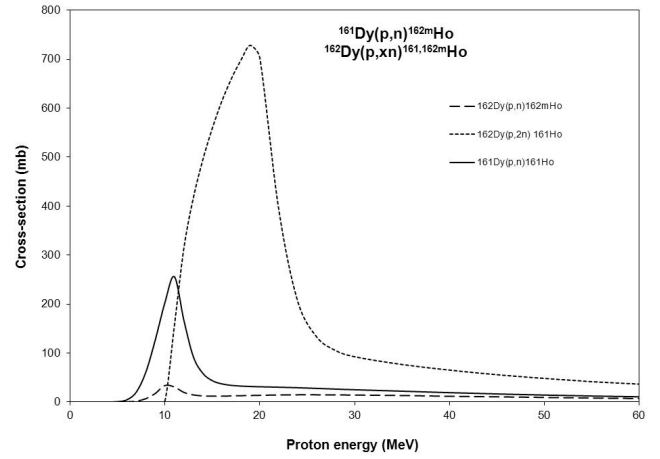
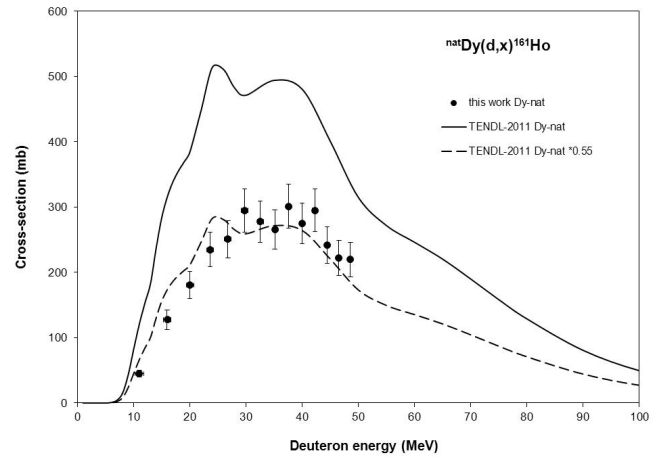
calculations. The numerical data important for further data evaluation are collected in Tables 4 and 5. In both cases the theoretical results reproduce exceptionally well the shape of the measured excitation functions, but an overestimation over the whole energy range is seen for the  $^{nat}\text{Dy}(p,x)^{161,162m}\text{Ho}$  and  $^{nat}\text{Dy}(d,x)^{161}\text{Ho}$  reactions. In case of the  $^{nat}\text{Dy}(d,x)^{162m}\text{Ho}$  the agreement of the maximum is acceptable. The numerical values of theoretical results by a factor of 0.7 in case of  $^{x}\text{Dy}(p,x)^{161,162m}\text{Ho}$  and of 0.55 in case of  $^{x}\text{Dy}(d,x)^{161}\text{Ho}$  should be multiplied as a rough estimation. There is no normalization for  $^{x}\text{Dy}(d,x)^{162m}\text{Ho}$  reaction. For further discussion we have normalized the theoretical cross-sections of the contributing reactions involved in  $^{161}\text{Ho}$  production with these factors. The comparison of the normalized TENDL 2011 cross-sections of the  $^{161}\text{Dy}(p,n)^{161}\text{Ho}$  and the  $^{162}\text{Dy}(p,2n)^{161}\text{Ho}$  reactions and the  $^{162}\text{Dy}(p,n)^{162m}\text{Ho}$  impurity reaction are shown in Fig. 4 and of the  $^{160}\text{Dy}(d,n)^{161}\text{Ho}$ , the  $^{161}\text{Dy}(d,2n)^{161}\text{Ho}$  reactions and the  $^{161}\text{Dy}(d,n)^{162m}\text{Ho}$  impurity reaction is presented in Fig 7.

**Table 3** Decay characteristics of the  $^{161}\text{Ho}$  and  $^{162m}\text{Ho}$  and Q-values of reactions for their productions)

Nuclide	Half-life	$E_\gamma$ (keV)	$I_\gamma$ (%)	Contributing reaction	Q-value (keV)	
$^{161}\text{Ho}$ $\epsilon$ : 100 % 7/2-	2.48 h	77.42	1.9	$^{161}\text{Dy}(p,n)$	-1640.64	
		103.05	103.05	$^{162}\text{Dy}(p,2n)$	-9837.63	
		157.26	0.49	$^{163}\text{Dy}(p,3n)$	-16108.65	
		175.42	0.43	$^{164}\text{Dy}(p,4n)$	-23766.77	
				$^{160}\text{Dy}(d,n)$	2589.18	
				$^{161}\text{Dy}(d,2n)$	-3865.2	
				$^{162}\text{Dy}(d,3n)$	-12062.2	
				$^{163}\text{Dy}(d,4n)$	-18333.21	
				$^{164}\text{Dy}(d,5n)$	-25991.33	
$^{162m}\text{Ho}$ IT: 62 % $\epsilon$ : 38 % 6- 105.87 keV	67.0 m	184.99	23.94	$^{162}\text{Dy}(p,n)$	-3027.91	
		282.86	10.27	$^{163}\text{Dy}(p,2n)$	-9298.92	
		937.17	10.44	$^{164}\text{Dy}(p,3n)$	-16957.05	
		1220.04	23.7			
				$^{161}\text{Dy}(d,n)$	2944.51	
				$^{162}\text{Dy}(d,2n)$	-5252.48	
				$^{163}\text{Dy}(d,3n)$	-11523.49	
				$^{164}\text{Dy}(d,4n)$	-19181.61	
$^{162g}\text{Ho}$ $\epsilon$ : 100 % 1+	15.0 m	80.7	8.0	$^{162}\text{Dy}(p,n)$	-2922.04	
		1319.75	3.82	$^{163}\text{Dy}(p,2n)$	-9193.05	
				$^{164}\text{Dy}(p,3n)$	-16851.18	
				$^{161}\text{Dy}(d,n)$	3050.38	
				$^{162}\text{Dy}(d,2n)$	-5146.61	
				$^{163}\text{Dy}(d,3n)$	-11417.62	
				$^{164}\text{Dy}(d,4n)$	-19075.74	

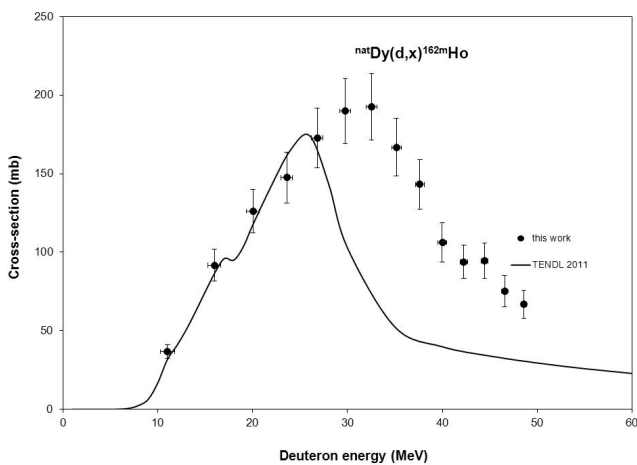
**Fig. 2** Experimental cross-sections of the  $^{nat}\text{Dy}(p,x)^{161}\text{Ho}$  reaction in comparison with the results of model calculations in TENDL 2011**Table 4** Measured cross-sections of the  $^{nat}\text{Dy}(p,x)^{161,162m}\text{Ho}$  reactions

E MeV	$^{161}\text{Ho}$		$^{162m}\text{Ho}$	
	$\sigma$ mb	$\pm\delta\sigma$	$\sigma$ mb	$\pm\delta\sigma$
35.3	253.5	34.8	34.7	5.7
33.8	246.2	35.6	46.9	5.9
32.3	293.4	39.0	55.6	7.3
30.8	285.5	38.1	82.6	10.2
29.2	265.0	35.2	103.4	11.5
27.5	214.8	33.2	113.6	14.6
25.7	239.8	32.2	114.6	13.1
23.8	239.2	34.1	118.6	13.4
21.9	248.9	28.1	111.1	12.3
19.7	226.1	25.5	93.0	10.4
17.4	178.8	20.6	80.8	9.0
14.8	156.1	21.1	73.0	8.0
11.9	122.3	14.1	49.0	5.4
8.2	39.2	5.8	15.3	1.7
4.3	5.7	1.7	0.8	0.1

**Fig. 3** Experimental cross-sections of the  $^{nat}\text{Dy}(p,x)^{162m}\text{Ho}$  reaction in comparison with the results of model calculations in TENDL 2011**Fig. 4** Experimental cross-sections of the  $^{nat}\text{Dy}(d,xn)^{161}\text{Ho}$  reaction in comparison with the results of model calculations in TENDL 2011**Fig. 5** Experimental cross-sections of the  $^{nat}\text{Dy}(d,xn)^{162m}\text{Ho}$  reaction in comparison with the results of model calculations in TENDL 2011

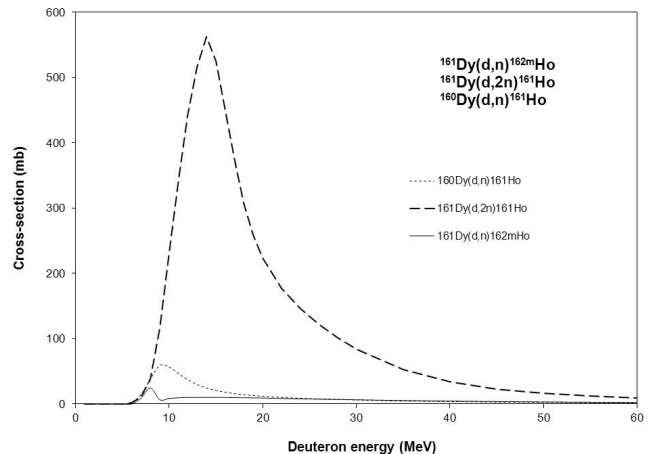
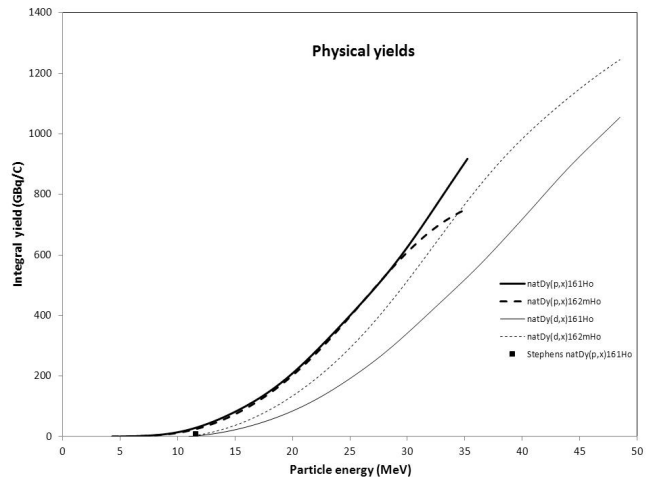
**Table 5** Measured cross-sections of the  $^{nat}\text{Dy}(\text{d},\text{x})^{161,162\text{m}}\text{Ho}$  reactions

E MeV	$^{161}\text{Ho}$		$^{162\text{m}}\text{Ho}$	
	$\sigma$ mb	$\pm\delta\sigma$	$\sigma$ mb	$\pm\delta\sigma$
48.6	219.9	26.6	66.7	9.0
46.5	222.2	26.9	75.2	10.0
44.4	242.0	28.1	94.4	11.2
42.3	295.2	33.1	93.9	10.8
40.0	274.8	31.3	106.1	12.5
37.6	301.0	33.7	143.2	15.7
35.1	265.8	29.8	166.8	18.4
32.5	277.7	31.3	192.5	21.1
29.8	295.1	33.1	189.9	20.8
26.8	250.9	28.3	172.8	19.0
23.6	234.9	26.3	147.5	16.3
20.0	181.0	20.5	126.1	13.9
16.0	127.5	14.7	91.7	10.1
11.0	45.0	5.5	36.6	4.2

**Fig. 6** Comparison of the cross-sections of the  $^{161}\text{Dy}(\text{p},\text{n})^{161}\text{Ho}$  and the  $^{162}\text{Dy}(\text{p},2\text{n})^{161}\text{Ho}$  reactions and the  $^{162}\text{Dy}(\text{p},\text{n})^{162\text{m}}\text{Ho}$  impurity reaction in TENDL 2011

### 3.2 Integral yields

The integral yields calculated on the basis of the normalized TENDL 2011 cross-sections for the  $^{nat}\text{Dy}(\text{p},\text{xn})^{161}\text{Ho}$ ,  $^{nat}\text{Dy}(\text{p},\text{xn})^{162\text{m}}\text{Ho}$ ,  $^{nat}\text{Dy}(\text{d},\text{xn})^{162\text{m}}\text{Ho}$  and  $^{nat}\text{Dy}(\text{d},\text{xn})^{162\text{m}}\text{Ho}$  production reactions are shown in Fig. 8. The calculated integral yield represents so called physical yield i.e. yield obtained in a short irradiation [19]. The  $^{nat}\text{Dy}(\text{p},\text{xn})^{161}\text{Ho}$  yields are compared with the experimental data of Stephens [5]. The value calculated by the Stephens' result for 11.6 MeV proton bombardment is significantly lower than our result, but it can be caused by the fact that the irradiation time was not published in that paper. Comparing the saturation activities, which are 1.8 GBq by Stephens (after 3.6 hours) and 1.89 GBq in our measurement/calculation, the agreement can be considered as good.

**Fig. 7** Comparison of the cross-sections of the  $^{160}\text{Dy}(\text{d},\text{n})^{161}\text{Ho}$  and the  $^{161}\text{Dy}(\text{d},2\text{n})^{161}\text{Ho}$  reactions and the  $^{161}\text{Dy}(\text{d},\text{n})^{162\text{m}}\text{Ho}$  impurity reaction in TENDL 2011**Fig. 8** Integral yields of the  $^{nat}\text{Dy}(\text{p},\text{xn})^{161}\text{Ho}$ ,  $^{nat}\text{Dy}(\text{p},\text{xn})^{162\text{m}}\text{Ho}$ ,  $^{nat}\text{Dy}(\text{d},\text{xn})^{162\text{m}}\text{Ho}$  and  $^{nat}\text{Dy}(\text{d},\text{xn})^{162\text{m}}\text{Ho}$  reactions

### 4 Comparison of production routes on different target materials

The main parameters of the selected low and medium energy reactions that can lead to production of  $^{161}\text{Ho}$  on different target materials are collected in Table 6. The excitation functions of the proton and deuteron routes are shown in Figs. 2-3 and Fig 4-5. Mukherjee [21] and Bonesso [22] reported earlier experimental cross-section data on  $^{159}\text{Tb}(\alpha,2\text{n})^{161}\text{Ho}$  and Mukherjee [21] and Singh [23] on total cross-section of and  $^{159}\text{Tb}(\alpha,2\text{n})^{162}\text{Ho}$ . The  $^{162\text{m}}\text{Ho}/^{162\text{g}}\text{Ho}$  isomeric ratio was measured by Tulinov [24], Baskova [25]. No experimental data were found for the  $^{159}\text{Tb}(\text{}^3\text{He},\text{n})^{161}\text{Ho}$  reaction. The experimental data from literature and the

theoretical excitation functions of the  $^{159}\text{Tb}(\alpha,2n)^{161}\text{Ho}$  and  $^{159}\text{Tb}(\alpha,n)^{162m}\text{Ho}$  reactions are shown in Fig. 9 and 10 respectively. The theoretical excitation functions of the  $^{159}\text{Tb}(\alpha,2n)^{161}\text{Ho}$  and  $^{159}\text{Tb}(n)^{162m}\text{Ho}$  and the  $^{159}\text{Tb}({}^3\text{He},n)^{161}\text{Ho}$  reactions are compared in Fig. 11. From the excitation functions of the above mentioned reactions the following conclusions can be drawn:

- The production yields for the  $^{162}\text{Dy}(p,2n)$  is the highest followed by the  $^{161}\text{Dy}(d,2n)$ ,  $^{159}\text{Tb}(\alpha,2n)$  and  $^{161}\text{Dy}(p,n)$
- No  $^{162m}\text{Ho}$  impurity is produced when using of  $^{159}\text{Tb}({}^3\text{He},n)$ ,  $^{161}\text{Dy}(p,n)$  and the  $^{160}\text{Dy}(d,n)$  reactions. Among them the  $^{161}\text{Dy}(p,n)$  reaction has the highest cross-section ( max 260 mb) followed by the  $^{160}\text{Dy}(d,n)$  reaction( max 60 mb) and the less productive  $^{159}\text{Tb}({}^3\text{He},n)$  ( max 1 mb)
- The element Tb is monoisotopic, relatively cheap and recovery is practically not necessary
- In case of proton and deuteron induced reactions highly enriched 160, 161 or 162 Dy targets are required
- The production cross-sections of the  $^{162m}\text{Ho}$  from  $^{169}\text{Tb}(\alpha,n)$ ,  $^{161}\text{Dy}(d,n)$  and  $^{162}\text{Dy}(d,n)$  are low
- The impurity level depends on the selected energy range. The ratio of the saturation yields of the main reaction and of competing impurity reaction is shown in Fig. 12 as a function of energy. In the production energy range the ratio is lower than 3
- The half-life of  $^{162m}\text{Ho}$  is three times shorter, therefore by using a short irradiation, the activity impurity level will reach 3%. But by using irradiations lasting two half-life of  $^{161}\text{Ho}$  and taking into account 1 hour needed for the chemical separation and the labeling process the impurity level of  $^{162m}\text{Ho}$  will be reduced to 1% by decay.

## 5 Summary and conclusions

The principal aim of this work was an investigation of the production possibility of the radiotherapy related  $^{161}\text{Ho}$ . We present first experimental cross-sections for  $^{nat}\text{Dy}(p,xn)^{161}\text{Ho}$ ,  $^{nat}\text{Dy}(p,xn)^{162m}\text{Ho}$ ,  $^{nat}\text{Dy}(d,x)^{161}\text{Ho}$  and  $^{nat}\text{Dy}(d,x)^{162m}\text{Ho}$  up to 40 and 50 MeV incident particle energies respectively. The TENDL 2011 theoretical data predict well the shape of the excitation functions but overestimate the absolute values with a nearly constant factor in the whole energy range. The comparison of the different production routes shows that for production of  $^{161}\text{Ho}$  with high radionuclide purity the  $^{161}\text{Dy}(p,n)^{161}\text{Ho}$ ,  $^{162}\text{Dy}(p,2n)$  and  $^{161}\text{Dy}(d,2n)$  reactions give the highest production yields. The  $^{162m}\text{Ho}$

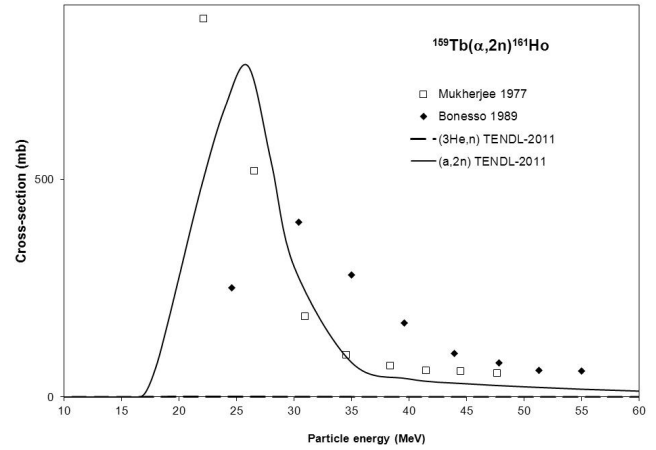


**Fig. 9** Experimental and theoretical cross-sections of the  $^{159}\text{Tb}(\alpha,2n)^{161}\text{Ho}$  reaction

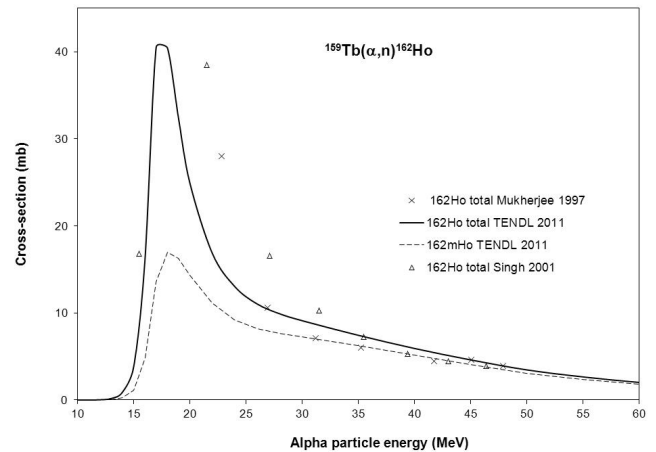


**Fig. 10** Experimental and theoretical cross-sections of the  $^{159}\text{Tb}(\alpha,n)^{162m}\text{Ho}$  reaction

radionuclide impurity level of the last two reactions however is significant. No enriched target material is necessary in case of  $^{159}\text{Tb}(\alpha,2n)$  (Tb is monoisotopic) but it requires accelerators having medium energy alpha particles. The  $^{159}\text{Tb}({}^3\text{He},n)$  and  $^{160}\text{Dy}(d,n)$  reactions have very low cross-sections, and accelerators disposing of  ${}^3\text{He}$  beam are rare and the  ${}^3\text{He}$  irradiation without recovery of  ${}^3\text{He}$  gas is expensive. On the basis of the production yields, the impurity levels and the requirements of the medical application the  $^{161}\text{Dy}(p,n)$  reaction is the production method of best choice.

**Acknowledgements** This work was performed in the frame of the HAS-FWO Vlaanderen (Hungary-Belgium) project. The authors acknowledge the support of the research project and of the respective institutions in providing the beam time and experimental facilities.

Table 6 Summary of the production parameters for selected reactions

Reaction	Q-value	Impurity reaction	Optimal energy range (MeV)	$^{161}\text{Ho}$ thick target yield (GBq/C)	Impurity level (%)	Optimal energy range at low impurity (MeV)	$^{161}\text{Ho}$ thick target yield (GBq/C)	Impurity level (%)
$^{159}\text{Tb}(\alpha,2n)^{161}\text{Ho}$	-16053.93	$^{159}\text{Tb}(\alpha,n)^{162m}\text{Ho}$	35-19	165	6	30-23	107	2.8
$^{159}\text{Tb}(^3\text{He},n)^{161}\text{Ho}$	4523.7	no	30-15		0			
$^{161}\text{Dy}(p,n)^{161}\text{Ho}$	-1640.64	no	15-8	132	0			
$^{162}\text{Dy}(p,2n)^{161}\text{Ho}$	-9837.63	$^{162}\text{Dy}(p,n)^{162m}\text{Ho}$	30-12	1459	8.5	22-15	868	4.6
$^{160}\text{Dy}(d,n)^{161}\text{Ho}$	2589.18	no	15-7	34	0			
$^{161}\text{Dy}(d,2n)^{161}\text{Ho}$	-3865.2	$^{161}\text{Dy}(d,n)^{162m}\text{Ho}$	30-16	1454	1.8	28-20	955	1.5

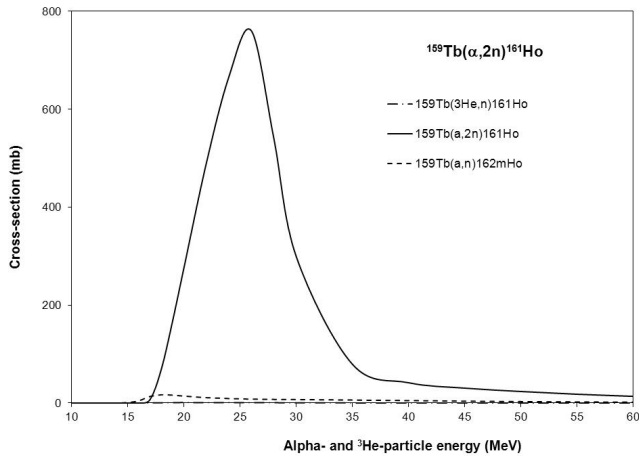


Fig. 11 Comparison of the cross-sections of the  $^{159}\text{Tb}(\alpha,2n)^{161}\text{Ho}$  and the  $^{159}\text{Tb}(^3\text{He},n)^{161}\text{Ho}$  reactions and the  $^{159}\text{Tb}(\alpha,n)^{162m}\text{Ho}$  impurity reaction (TENDL 2011)

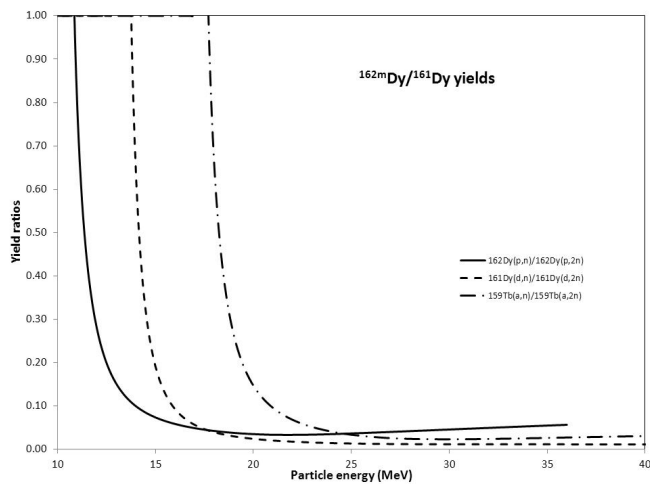


Fig. 12 The ratio of the saturation yield of the main reaction and the satellite impurity reaction

## References

1. A.J. Koning, D. Rochman. Talys-based evaluated nuclear data library version 4 (2011)
2. H. Uusijarvi, P. Bernhardt, F. Rosch, H.R. Maecke, E. Forssell-Aronsson, Journal of Nuclear Medicine **47**(5), 807 (2006)
3. F. Rosch, Radiochimica Acta **95**(6), 303 (2007)
4. M. Neves, A. Kling, A. Oliveira, Journal of Radioanalytical and Nuclear Chemistry **266**(3), 377 (2005)
5. B.J. Stephens,  $^{161}\text{Ho}$  + iudr: optimized photon activation therapy. Ph.D. thesis (2010)
6. B.J. Stephens, M.H. Mendenhall, Applied Radiation and Isotopes **68**(10), 1928 (2010)
7. S. Takács, F. Tárkányi, A. Hermanne, R.A. Rebeles, Nuclear Instruments & Methods in Physics Research Section B-Beam Interactions with Materials and Atoms **269**(23), 2824 (2011)
8. F. Tárkányi, F. Ditrói, S. Takács, B. Király, A. Hermanne, M. Sonck, M. Baba, A.V. Ignatyuk, Nuclear Instruments & Methods in Physics Research Section B-Beam Interactions with Materials and Atoms **274**, 1 (2012)
9. A. Hermanne, F. Tárkányi, F. Ditrói, S. Takács, R.A. Rebeles, M.S. Uddin, M. Hagiwara, M. Baba, Y. Shubin, S.F. Kovalev, Nuclear Instruments & Methods in Physics Research Section B-Beam Interactions with Materials and Atoms **247**(2), 180 (2006)
10. M.S. Uddin, M. Hagiwara, M. Baba, F. Trknyi, F. Ditrói, Applied Radiation and Isotopes **63**(3), 367 (2005)
11. F. Tárkányi, F. Ditrói, S. Takács, J. Csikai, A. Hermanne, M.S. Uddin, M. Hagiwara, M. Baba, Y.N. Shubin, A.I. Dityuk, Nuclear Instruments & Methods in Physics Research Section B-Beam Interactions with Materials and Atoms **226**(4), 473 (2004)
12. F. Tárkányi, S. Takács, K. Gul, A. Hermanne, M.G. Mustafa, M. Nortier, P. Oblozinsky, S.M. Qaim, B. Scholten, Y.N. Shubin, Z. Youxiang, Beam monitor reactions (chapter 4). charged particle cross-section database for medical radioisotope production: diagnostic radioisotopes and monitor reactions. Tech. rep., IAEA (2001)
13. Canberra. <http://www.canberra.com/products/radiochemistry-lab/genie-2000-software.asp>.
14. G. Székely, Computer Physics Communications **34**(3), 313 (1985)
15. F. Tárkányi, F. Szelecsényi, S. Takács, Acta Radiologica, Supplementum **376**, 72 (1991)
16. NuDat. Nudat 2.5 database <http://www.nndc.bnl.gov/nudat2/> (2011)
17. B. Pritychenko, A. Sonzogni. Q-value calculator (2003)
18. H.H. Andersen, J.F. Ziegler, *Hydrogen stopping powers and ranges in all elements. The Stopping and ranges of ions in matter, Volume 3*. The Stopping and ranges of ions in matter (Pergamon Press, New York, 1977)
19. I.B. of-Weights-and Measures, *Guide to the expression of uncertainty in measurement*, 1st edn. (International Organization for Standardization, Genève, Switzerland, 1993)
20. M. Bonardi. The contribution to nuclear data for biomedical radioisotope production from the milan cyclotron facility (1987)
21. S. Mukherjee, B.B. Kumar, M.H. Rashid, S.N. Chintalapudi, Physical Review C **55**(5), 2556 (1997)

22. O. Bonesso, H.O. Mosca, S.J. Nassiff, *Journal of Radioanalytical and Nuclear Chemistry-Letters* **137**(1), 29 (1989)
23. N.L. Singh, M.S. Gadkari, *Acta Physica Slovaca* **51**(5), 271 (2001)
24. A.F. Tulinov, T.V. Chuvilskaya, L.Y. Shavtvalov, *Bull.Acad.Sci.USSR, Phys.Ser.* **53**(11), 209 (1989)
25. K.A. Baskova, Y.V. Krivonogov, B.M. Makuni, E.A. Skakun, T.V. Chugai, L.Y. Shavtvalov. Isomer yields of 73-m,-g se, 162-m,-g ho and 183-m,-g os in (alpha,n) reactions (1985)